


Article

Development of Neutral Red as a pH/pCO₂ Luminescent Sensor for Biological Systems

Megan N. Ericson [†], Sindhu K. Shankar [†], Laya M. Chahine, Mohammad A. Omary , Ione Hunt von Herbing ^{*} and Sreekar B. Marpu ^{*}

Department of Chemistry, University of North Texas, Denton, TX 76201, USA; meganericson2@my.unt.edu (M.N.E.); sindhukonanurshankar@my.unt.edu (S.K.S.); lchahine9@gmail.com (L.M.C.); mohammad.omary@unt.edu (M.A.O.)

^{*} Correspondence: ione.huntvonherbing@unt.edu (I.H.v.H.); sreekarbabu.marpu@unt.edu (S.B.M.); Tel.: +940-565-3595 (I.H.v.H.); +940-565-4850 (S.B.M.)

[†] M.N.E. and S.K.S. are equal contributing authors.

Abstract: Neutral Red (NR), a eurydine dye, is often used for staining living cells, but we demonstrated for the first time that NR can also serve as a CO₂ sensor, because of NR's unique optical properties, which change with dissolved carbon dioxide (dCO₂) concentrations. In the present study, optical sensitivity of NR was quantified as a function of changes in absorption and emission spectra to dCO₂ in a pH 7.3 buffer medium at eight dCO₂ concentrations. NR exhibited a response time of two minutes for equilibration in pure N₂ to 100% CO₂ with an ~200% percent change (%Δ) in emission intensity and >400%Δ in absorbance, with full reversibility. Important to its application to biological systems, NR exhibited zero sensitivity to dissolved oxygen, which has routinely caused interference for CO₂ measurements. NR exhibited pH sensitive emission and excitation energies with dual excitation wavelengths at 455 nm and 540 nm, and a single emission at 640 nm. The CO₂ sensing properties of NR were benchmarked by a comparison to pyranine (8-hydroxypyrene-1, 3, 6-trisulfonic acid trisodium salt) (HPTS). Future studies will evaluate the feasibility of NR as an intracellular in vivo pCO₂ sensor in aquatic organisms critically impacted by increasing global CO₂ levels.

Keywords: chemo sensor; fluorescence; absorption; emission; sensing; detection; carbon dioxide



Citation: Ericson, M.N.; Shankar, S.K.; Chahine, L.M.; Omary, M.A.; Herbing, I.H.v.; Marpu, S.B. Development of Neutral Red as a pH/pCO₂ Luminescent Sensor for Biological Systems. *Chemosensors* **2021**, *9*, 210. <https://doi.org/10.3390/chemosensors9080210>

Academic Editor: José Manuel Costa Fernández

Received: 22 June 2021

Accepted: 28 July 2021

Published: 5 August 2021

Publisher's Note: MDPI stays neutral with regard to jurisdictional claims in published maps and institutional affiliations.



Copyright: © 2021 by the authors. Licensee MDPI, Basel, Switzerland. This article is an open access article distributed under the terms and conditions of the Creative Commons Attribution (CC BY) license (<https://creativecommons.org/licenses/by/4.0/>).

1. Introduction

The development of optical carbon dioxide (CO₂) sensors is an expanding area of analytical science because of the demand for inexpensive and efficient devices for use in engineering and medicine [1]. CO₂ sensors are essential for the detection of environmental changes related to global temperature increases such as ocean acidification and for use in monitoring dissolved CO₂ levels in stagnant rivers and lakes [1–4]. Further, CO₂ sensors are used in the monitoring of internal blood gases in routine medical practice to evaluate human health [1,5], because when too much CO₂ accumulates in the blood, disruption of the regulation of gas exchange in the lungs can affect cardiac and neurological functions as well as downstream immune responses [5,6]. While there are several CO₂ sensitive optical materials available most of them have limitations, which include high cost, sensitivity to electrical interference, sensitivity to pH changes and acidic or basic gases, and often have slow response and recovery times [1]. There is a clear and immediate need, therefore, to develop alternative molecular systems for CO₂ detection. In the present study, we offer a novel CO₂ sensor, Neutral Red (NR), and provide evidence of NR's efficacy as a new pH/pCO₂ luminescent sensor to measure dCO₂. Indirect sensing of CO₂ involves the measurement of changes in CO₂ concentrations and NR, a cellular stain, responds to changes in dissolved (dCO₂) under different pHs and external CO₂ concentrations. Measuring changes in CO₂ concentration based on the changes in pH of the medium has been a method used primarily by the Severinghaus electrode [1,7].

While there are some advantages, including high accuracy and stability, for using Severinghaus electrodes to measure CO₂ concentration, the disadvantages far outweigh the advantages. Some common disadvantages of Severinghaus electrodes include high-cost, bulkiness, slow response and recovery times, contamination of reference electrode, liquid junction fouling, and high maintenance. Severinghaus electrodes are also vulnerable to electrical interferences, the presence of acidic and basic gases, changes in osmotic pressure and therefore salt conditions. [1,8–10]. Alternative CO₂ sensors to the Severinghaus devices are needed, which are inexpensive, portable, robust, with rapid response times and that can monitor analyte concentrations continuously. For these reasons, CO₂ sensors that function based on optical signal (absorbance or fluorescence) changes are of high interest. Optical CO₂ sensors come in two forms: (1) colorimetric/absorption-based, and (2) luminescence-based, and can potentially replace electrodes equipped with pH indicators. Of the two forms, luminescent sensors are more desirable because of their higher sensitivity compared to colorimetric dyes as the pKa of the sensing material or colorimetric/fluorescent dye will play a major role in the selection of the sensor materials. A colorimetric/luminescent dye with a pKa value close to the first dissociation constant of carbonic acid is a good choice for effective CO₂ detection. For intracellular studies in biological systems, the range of detection should bracket the pH range typical of a live biological cell, i.e., pH 7.0 to 7.4 [11]. It is therefore critically important that for a CO₂ sensor to be efficient for use in biological systems, the sensor signal must be non-responsive to dissolved oxygen concentrations present in the atmosphere and the water [12].

In the present study, we provide evidence that NR can reliably measure dissolved CO₂ (dCO₂) in buffered media. While NR has been commonly used as a non-fluorescent pH indicator and biological stain, it also exhibits concentration-dependent optical properties, is non-fluorescent at concentrations higher than 10^{−4} M, with a pH sensitive emission detectable at concentrations of <10^{−4} M [13–15]. The chemical structure and effect of pH on the chemistry of NR is shown in Figure 1. NR exhibits pH-dependent dual excitation/absorption peaks at 455 and 540 nm. The fluorescent emission peak maximum is not altered with pH and is centered at 640 nm from pHs ranging from 5.9 to 8.2. The orange-red emission at 640 nm is considerably red-shifted from the auto-fluorescence of many biological organelles and thereby expected to exhibit minimized background interference, which is useful for intracellular CO₂ studies. The universal cellular fluorophores—NADPH, proteins, and flavins exhibit mostly blue and green emission [16,17]. The pKa of neutral red is 6.9, which lies near to the first pKa of carbonic acid of 6.35, and because the pKa of NR is near to neutral pH, this suggests that NR will serve as a good candidate as a CO₂ sensor especially for biological systems. NR as a pH luminescent sensor for environmental and biological applications has the promising additional property of very low toxicity [18], based on the fact that NR has been certified as a biological stain and is well known as a method for determining cell viability through the staining of lysosomes and chromatin staining [14,15,18]. In an eco-toxicological safety study by Kastury et al. (2015), acute toxicity values of NR were determined to lie between 2.5 × 10^{−4} M to 0.01 M [19,20]. In the present study, all experiments were conducted at NR concentrations below 10^{−5} M.

Many past studies of fluorescent CO₂ sensors used sensors made from pyranine (8-hydroxypyrene-1, 3, 6-trisulfonic acid trisodium salt (HPTS) with a pKa of 7.3 [1]. HPTS is ideal for sensing pCO₂ because as with NR, HPTS exhibits pH-dependent dual excitation and a single emission spectrum with excitation/absorption at 405 nm at pHs below the pKa and exhibited a red-shifted 455 nm excitation/absorption at pHs above the pKa of the system. HPTS peak emission is centered at 515 nm and is unaffected by the pH of the medium between the pH range of 6.5 to 8.0. The structure of HPTS in acidic and basic conditions is in the Figure S1. The emission and excitation spectra at different pHs along with changes in the color of HPTS in buffer solution under ambient and under UV light irradiation are shown in Figure S2. Several studies have demonstrated that response and recovery times of optical sensors vary with fabrication as well as experimental conditions including type of buffer, pH, dye concentration, and coating thickness [1]. HPTS is a

bicarbonate buffer and will detect concentrations as low as 5% CO₂ in 15 s with a recovery time of 30 s [7]. HPTS is also known to have low toxicity, although this property has not been rigorously investigated [12]. A major limitation of HPTS for intracellular biological studies is its lack of cell permeability [12], compared to NR [18]. While our major goal in the present study was to establish the CO₂ sensing properties of NR, some additional experimental studies were performed to compare and contrast the CO₂ sensing properties of NR with the well-established HPTS system. These studies include comparing the NR vs. HPTS under the same experimental conditions of differing dCO₂ and pH to determine differences in sensor sensitivity, response time, and reversibility.

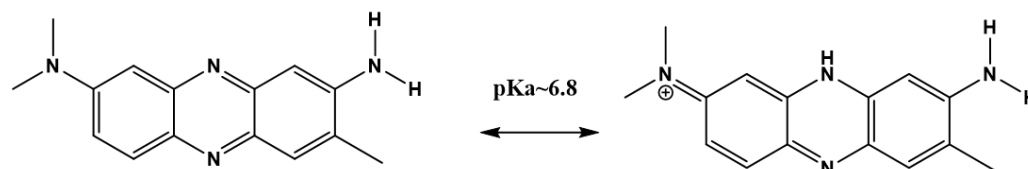


Figure 1. The chemical structure of NR in basic and acidic media, respectively.

2. Materials and Methods

Six different 1 mM fresh phosphate-buffered solutions of pH, 5.5, 6, 6.5, 7, 7.5, and 8 were prepared by adding different ratios of NaH₂PO₄ and Na₂HPO₄ to de-ionized (DI) water. An 8×10^{-4} M aqueous stock solution of neutral red (NR) was prepared by dissolving NR in DI water and different pH solutions of NR in phosphate-buffered solution were prepared by adding 0.4 mL of the NR stock solution to each of the six phosphate-buffered solutions of the desired pH (as mentioned above), resulting in a final NR solution concentration of 3.1×10^{-5} M. It should be noted that on addition of the NR stock solution to the pH phosphate-buffered solutions, the final pH of the samples increased slightly to reach a final pH of, 5.9, 6.4, 6.8, 7.3, 7.8 and 8.2. For comparison, solutions of HPTS were prepared using the same methods as with NR. All (NR and HPTS) solutions were investigated to determine the effects of pH on their fluorescence properties.

Different concentrations of CO₂ and N₂ gas mixtures were used in the experiments to determine NR's ability to detect changes in dCO₂ in a buffer medium. To arrive at different gas concentrations, pre-mixed cylinders of CO₂/N₂ gas were purchased with the following gas ratios, 2/98, 5/95, 6/94, 10/90, 25/75, 50/50 and 100/0 or, 2%, 5%, 6%, 10%, 25%, 50% and 100% CO₂, respectively. The 10 mL NR buffer solution at pH 7.3 was selected to be used for the CO₂ purging studies (Figure 2). Purging studies consisted of the following steps, (1) the test sample was first de-aerated by purging it with N₂ followed by saturation with 100% CO₂, (2) the treated solution was then brought back to its initial state by purging the sample with 100% N₂ followed by, (3) purging with the pre-mixed gases of, 2%, 5%, 6%, 10%, 25%, 50% and 100% CO₂ from the pre-mixed cylinders and then neutralization by purging with 100% N₂ (Figure 2). Fluorescence spectra were recorded using PTI Quanta Master Model QM-4, with a 75-watt Xenon arc lamp source and photomultiplier tube detector, scanning spectrofluorometric and absorption spectra are recorded using the PerkinElmer Lambda 900 UV/VIS/NIR spectrophotometer.

Following the fluorescence studies, blanketing studies were performed using 10 mL of 3.1×10^{-5} M NR solution at pH 7.3, on a Zeiss Axio Observer Z1 epifluorescent microscope equipped with an incubation chamber in which different atmospheric mixtures of CO₂/N₂ gases could be maintained for several hours if necessary. The microscope setup and environmental chamber are shown in Figures 3 and S3. As in the fluorometer, different concentrations of CO₂ gas were tested to further characterize the sensitivity of NR using epifluorescence microscopy. For each blanketing study, a NR sample was first purged with 100% CO₂ and then brought back to neutral by purging with 100% N₂. The desired CO₂ concentration within the environmental chamber was obtained by mixing the gases from 100% CO₂ cylinder with different amounts of room atmosphere air, (about 78% N₂), to obtain 2%, 4%, and 6% final CO₂ concentrations. Due to technical limitations,

the maximum CO₂ concentration attained in the incubation chamber was 6%. Images from the Zeiss microscope were captured using Zeiss image software and were taken for 60 min at 10 min intervals during CO₂ exposure and at 20 min intervals during reversibility studies. For the 100% CO₂ measurements, the sample was directly purged with CO₂ gas and then images were recorded.

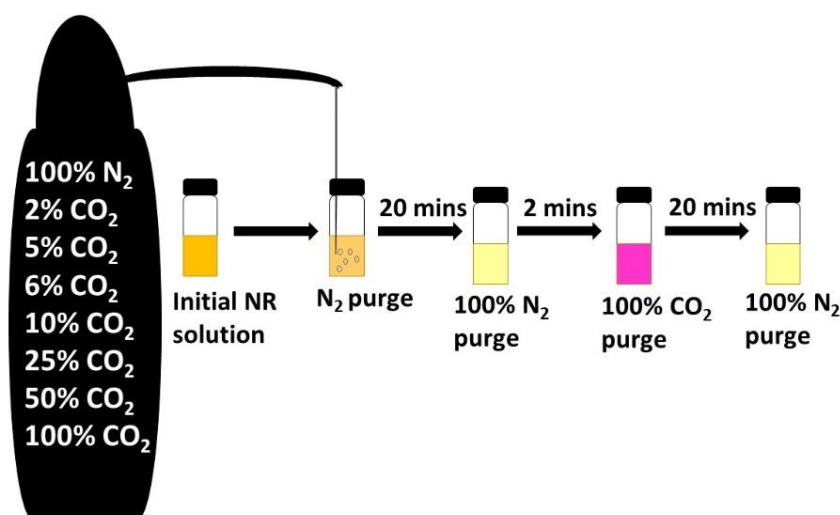


Figure 2. Schematics showing the sequential steps for purging studies of Neutral Red (NR) using different gas mixtures of CO₂/N₂ in a fluorometer.



Figure 3. A complete fluorescent microscope setup is shown. (A) Set-up of the Zeiss Axio observer Z1 epifluorescent microscope, (B) 100% CO₂ and N₂ gas tanks and mixing modules and, (C) incubation chamber.

Calibrations existed within the microscope to determine and maintain the desired final atmospheric CO₂ concentrations during the experiments [21,22]. Epifluorescence of each sample was recorded when the sample solution was blanketed with three different concentrations of CO₂ gas (2%, 4%, 6%) and exposed to light passed through a rhodamine band-pass (BP) filter with an excitation of 546/12 and an emission of 575–640 nm [23]. The rhodamine band-pass (BP) filter was selected because of the overlap with the excitation 540 nm and emission 640 nm, peaks of the NR solution system. For the 100% CO₂ studies, the NR sample was removed from the incubation chamber and purged with 100% CO₂ gas externally because concentrations could not reach 100% CO₂ within the incubation chamber. All microscopic images were analyzed using ImageJ [24].

Table 1 shows the % partial pressure, kPa and mm of Hg, and molar concentrations of CO₂ gas used in this study. The % values were either directly obtained from the gas cylinder manufacturer or controlled via the Zeiss Axiovert mixing modules, while partial pressure and molar concentration values in the solution were directly calculated.

Table 1. List of CO₂ concentrations used in this study.

Percent CO ₂ (%)	pCO ₂ (kPa)	pCO ₂ (mm Hg)	dCO ₂ Concentration (mM)
2	2.03	15.22	0.68
4	4.05	30.37	1.36
5	5.06	37.96	1.70
6	6.08	45.60	2.04
10	10.13	75.98	3.40
25	25.33	189.95	8.50
50	50.66	379.90	17.00
100	101.32	759.96	34.00

3. Results and Discussion

Effects of pH on emission and excitation spectra of the NR solution were tested before determining the effects of different concentrations of dissolved CO₂ on NR's optical properties. Results from the pH experiments on NR in solution showed clear pH dependence (Figure 4A–C). Specifically, while a broad excitation band at 455 nm was observed from pHs of 7.3 to 8.2, at lower pHs 5.9 to 6.8 the excitation band red-shifted to 540 nm. In short, as pH was reduced from 8.2 to 5.9, the orange-red emission, which had a peak maximum at 640 nm, exhibited a 50% increase in intensity when excited with a single wavelength at 540 nm (Figure 4A). The dual excitation characteristic of NR is specifically useful for a good optical sensor because dual excitations can help overcome background interference and help with baseline corrections during the calibration of the sensor. The Xenon arc lamp has a wide excitation wavelength range (200–800 nm) which benefits the study of molecules with multiple excitation wavelengths. All photoluminescence studies reported here are monitored at an excitation wavelength of 540 nm. The optical properties of NR in a phosphate-buffered solution, therefore, were sensitive to pH changes between 6.0–8.5 and thus appropriate for dCO₂ studies in living organisms. The pK_a of the NR solution was calculated from an emission (I/I_0 at 640 nm) vs. pH plot and was determined to be 6.9 (Figure 4C).

Determination of the effects of dCO₂ on NR in a phosphate-buffered solution with a pH of 7.3 followed the pH experiments. A buffer solution with a pH of 7.3 was selected for the experiments because a pH of 7.3 is common in human blood. For example, arteries and veins carry blood between a pH of 7.2–7.4, the shift in pH responsible for the ability of hemoglobin to transport both O₂ and CO₂ and blood-oxygen dissociation curves in humans and is known as the Bohr Effect [25]. In the dCO₂ experiments, the NR buffered phosphate solution was initially saturated with 100% CO₂ gas for equilibration followed by purging it with 100% N₂. Responses and reversibility times were determined to be about 2 min and 10 min, respectively. After saturation with 100% CO₂ gas, absorption and emission data for the NR buffered phosphate solution was recorded when it was exposed to different concentrations of CO₂ gas (2%, 6%, 10%, 25%, 50%, and 100%) (Figures 5 and 6). In Figure 5A, NR buffered phosphate solution exhibited a 433.6% increase in absorbance signal at 540 nm when switched from 100% N₂ to 100% CO₂. At the lowest concentration of 2% CO₂ (0.68 mM), there was a 149.5% increase in absorbance signal at 540 nm and the absorbance at 540 nm and absorption spectra are completely reversible when gas mixtures were switched from pure N₂ to 100% CO₂ followed by purging with pure N₂ (Figure 5B). As the dCO₂ concentration is increased, an isosbestic point was observed at around 470 nm in Figures 4A, 5A and 6A indicated by '*'. The isosbestic point represents the presence of both the acidic and basic forms of NR, at equilibrium.

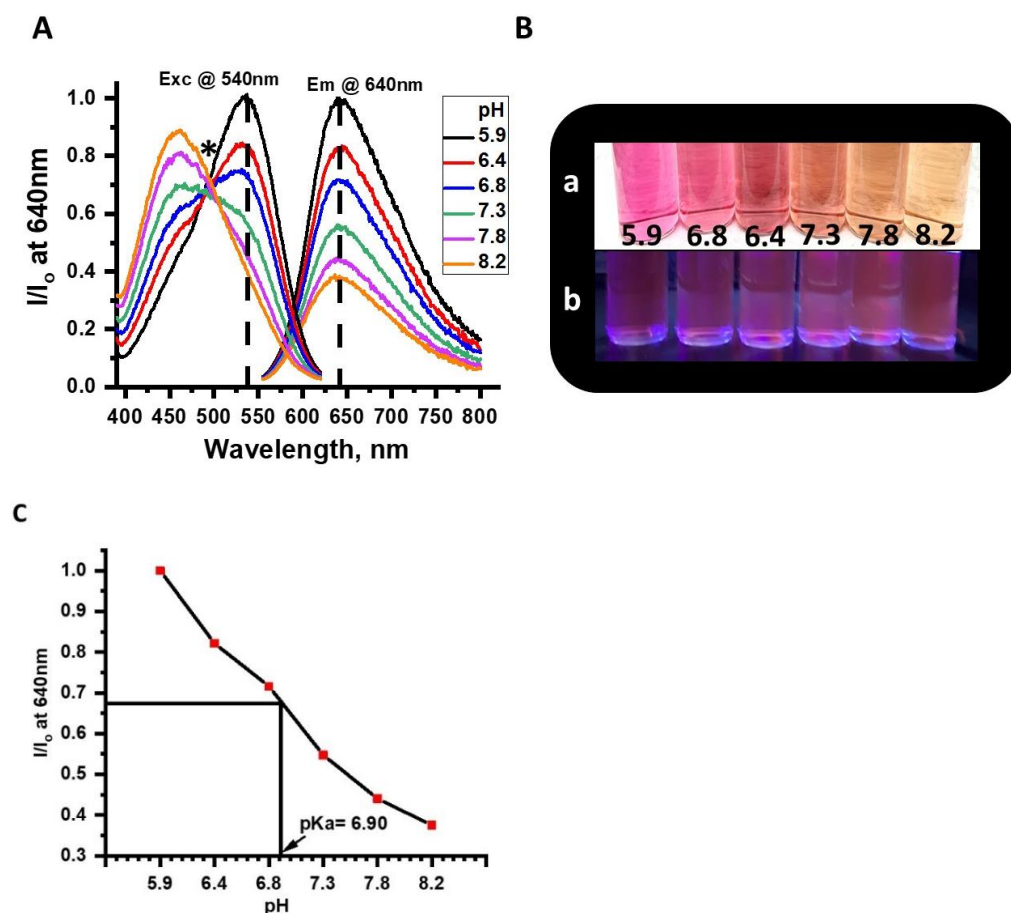


Figure 4. Changes in fluorescence of NR solution at different pH, (A) Excitation and emission spectra of NR buffer solutions recorded at 640 nm and 540 nm excitation wavelengths at pH values ranging from 5.9 to 8.2. The “*” represents the isosbestic point at around 470 nm. (B) Changes in physical and emission color of the complex with the respective pH of the NR buffer solutions, (a) Under ambient light, and (b) Under UV irradiation. (C) Emission intensity changes vs. pH at 640 nm wavelength for the same solutions. The arrow points at the pKa of the NR solution.

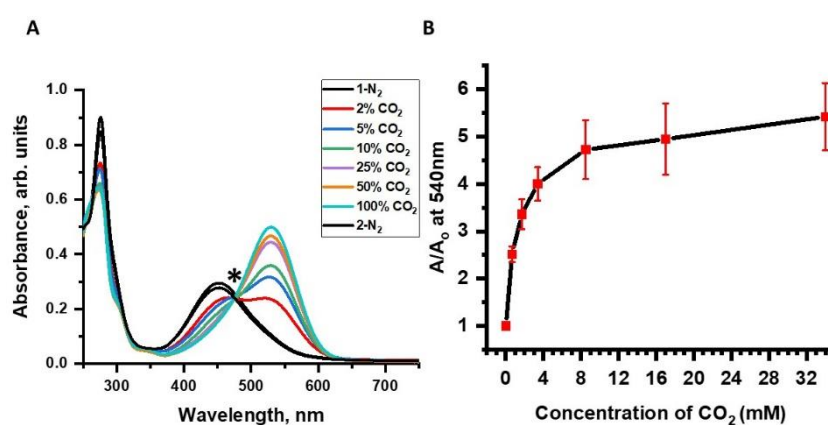


Figure 5. Changes in absorption of NR buffer solution (pH 7.3) purged with different concentrations of CO_2 gas (0.0 mM, 0.68 mM, 1.7 mM, 3.4 mM, 8.5 mM, 17.0 mM, 34.0 mM—0%, 2%, 5%, 10%, 25%, 50%, and 100%, respectively). (A) Changes in full absorption spectra. The “*” represents the isosbestic point at around 470 nm. (B) Changes in absorption signal vs. pH at 540 nm wavelength for one cycle at different gas concentrations.

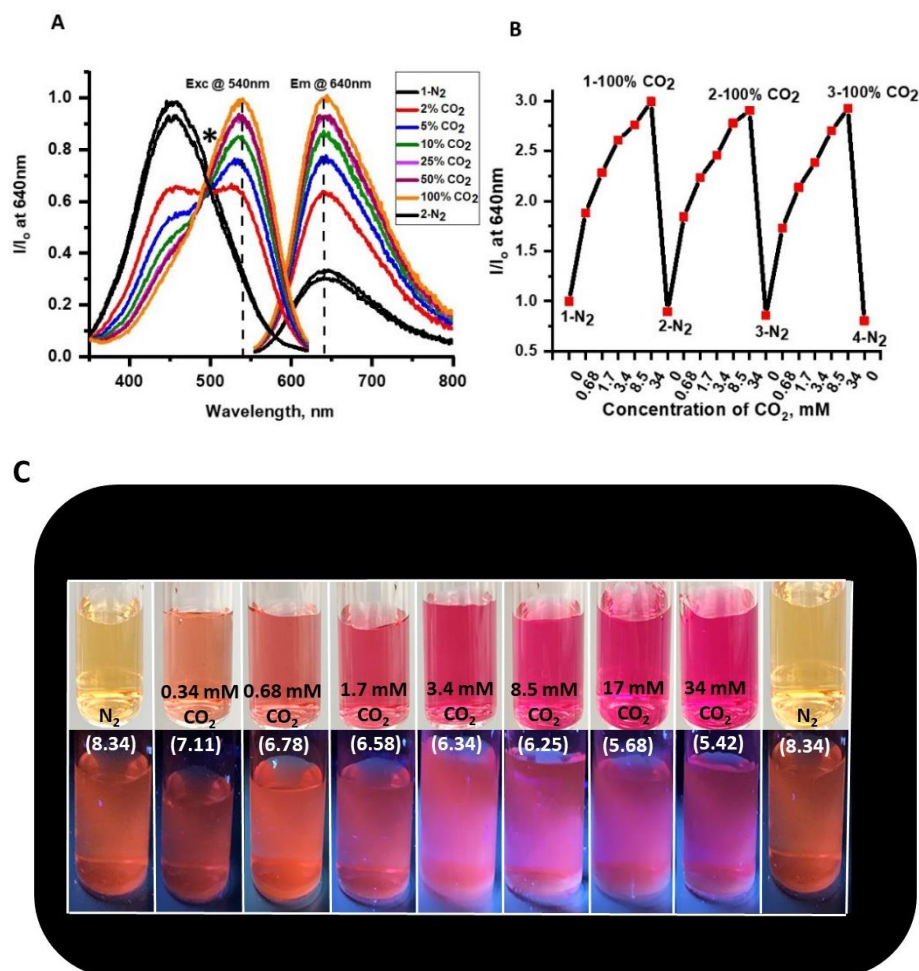


Figure 6. Changes in fluorescence of NR buffer solution at pH 7.3 purged with different concentrations of CO₂ gas (0.0 mM, 0.68 mM, 1.7 mM, 3.4 mM, 8.5 mM, 17.0 mM, 34.0 mM—0%, 2%, 5%, 10%, 25%, 50%, and 100%, respectively). (A) Changes in complete emission and excitation spectra. The '*' represents the isosbestic point at around 470 nm. (B) Changes in emission signal at 640 nm wavelength for 3 cycles of purging. (C) Changes in color of the solution under ambient light (top) and under UV excitation (bottom), the pH value of the solution is placed in parenthesis.

To further the development of a photo-luminescent CO₂ sensor and provide additional evidence for the significant changes observed in the absorbance of the NR solution under different concentrations of CO₂ gas, a series of fluorescence studies were conducted (Figure 6). The NR solution showed significant shifts in emission intensity at pH 7.3 when purged with different concentrations of dissolved CO₂, 2% (0.68 mM), 5% (1.7 mM), 10% (3.4 mM), 25% (8.5 mM), 50% (17 mM) and, 100% (34.0 mM) (Figure 6A). The NR solution exhibited > 10% signal change in absorbance as well as emission intensity at concentrations from 0 mM dCO₂. From these results, we concluded that changes in absorbance are greater than changes in emission. We suggest that the higher sensitivity of absorbance was due to an inner filter effect from the chromophore resulting in weaker fluorescence compared to its absorbance. Additionally, NR is known to exhibit self-quenching at higher concentrations, explaining the smaller changes in emission intensity vs. absorbance when exposed to dCO₂.

Figure 6B showed the drift in optical signal for three sensing cycles. Comparing emission intensities of different cycles at 100% (34 mM) dCO₂, I/I₀ values drifted no more than 3.05% and less than 24.2% at 0% (0 mM) dCO₂ highlighting the stability of NR system for dCO₂ sensor studies. Further, the NR solution also exhibited changes in absorbance and emission intensity upon exposure to different concentrations of dCO₂ and exhibited

reversibility upon purging with N₂ gas (Figures 4 and 5). In Figure 6C, clear changes in physical and emission color of the NR solution at different concentrations of CO₂ gas were observed and the % signal changes at different concentrations of dCO₂ for emission and absorption for NR solution are summarized in Table 2. Based on the changes in A/A_0 and using the 10% signal change rule the NR system can detect less than 0.68 mM dCO₂, and based on changes in I/I_0 , the NR solution can detect as low as 2.0 mM dCO₂ in a buffer media of pH 7.3. Complete information regarding the sensitivity of the complex between any two concentrations of the gases is given in Table S1.

For the NR solution, emission results from both the fluorometer and the epifluorescence microscope studies showed that the NR has a high potential to be used as a CO₂ sensor in in vivo biological studies (Figure 7). Data from the fluorometer and the epifluorescence microscope studies are compared to illustrate the differences in data calibration between the two instruments and to determine whether a single calibration can be used for both measurements. Data shown in Table 2 illustrated quite clearly that the emission intensity signal changes at a given CO₂ concentration were much higher from the fluorometer than from the epifluorescence microscope. The higher emission intensity changes and better sensitivity measurements from the fluorometer resulted from the higher inherent sensitivity of the fluorometer and from differences in the CO₂ exposure method. In addition, the NR optical signal did not exhibit sensitivity to dissolved O₂ gas (refer to Figure S4). This is important for an effective CO₂ sensor as interference caused by O₂ in the spectroscopic measurements is common due to the need for O₂ in all living aerobic systems.

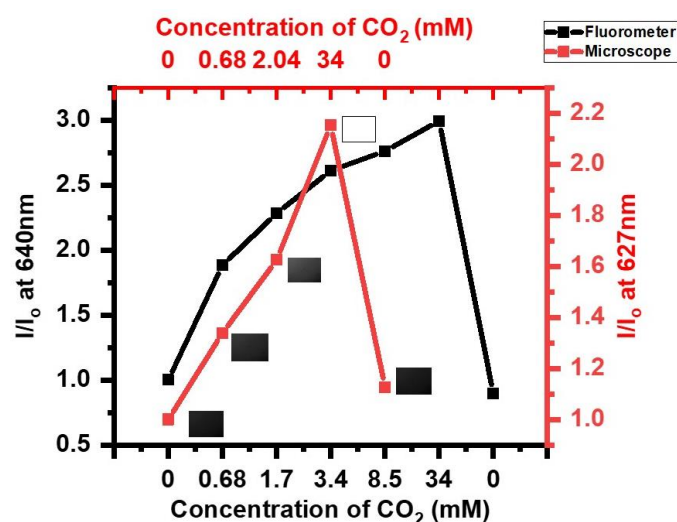


Figure 7. Changes in emission intensity (I/I_0) for NR solution with respect to different CO₂ levels as measured by the spectrofluorometer and epifluorescent microscope. The inset pictures show the relative emission brightness of the sample at different CO₂ concentrations. The inset images are the final, saturated fluorescent images of samples at different gas concentrations monitored on the epifluorescent microscope. Before saturation, images are taken at 10 min intervals during CO₂ exposure and at 20 min intervals during N₂ reversibility.

After determining the CO₂ sensing properties of NR solution in phosphate buffer media, the sensing properties of NR solution were compared and benchmarked against HPTS in the same media and pH as NR (Figure 8). For fluorescence measurements, HPTS was excited at 455 nm and changes in fluorescence emission signals were recorded for HPTS to compare response times, signal drift and percent emission signal changes with those of NR (Table 3). Results showed that the NR solution optical signal exhibited faster responses and recovery times compared to HPTS. Specifically, the NR solution exhibited emission signal changes from 0 mM to 0.68 mM, 0.68 mM to 2.04 mM, 2.04 mM to 3.40 mM, 3.4 mM to 34.0 mM of dCO₂, in 1/4, 2/3, 1/6, and 1/4 less time, respectively, than HPTS.

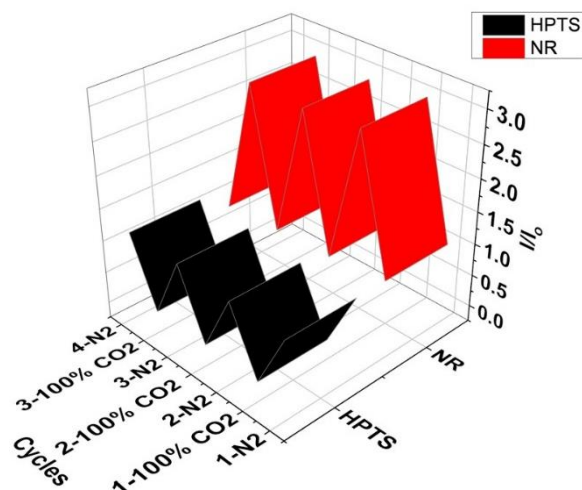


Figure 8. HPTS and NR purging cycles used to calculate the signal drift. Both HPTS and NR solutions are studied under similar experimental conditions and irradiated at a 455 nm and 540 nm excitation wavelengths, respectively.

Table 2. Carbon dioxide sensitivity numbers reported from absorbance/UV-Vis data, fluorescence data acquired using the spectrofluorometer, and epifluorescence using the Zeiss epifluorescence microscope. The concentrations of gases for epifluorescence studies were selected based on the technical limitation of the microscope gas chamber.

dCO ₂ Change (mM)	Absorbance		Fluorescence		Epifluorescence *	
	% Signal Change	Fold-Increase	% Signal Change	Fold-Increase	% Signal Change	Fold-Increase
0→0.68	149.50	2.50	88.29	1.88	33.81	1.34
0→1.70	232.10	3.32	128.32	2.28	N/A	N/A
0→2.04	N/A	N/A	N/A	N/A	62	1.63
0→3.40	296.00	3.96	161.10	2.61	N/A	N/A
0→8.50	365.20	4.65	176.21	2.76	N/A	N/A
0→17.00	385.80	4.86	176.35	2.76	N/A	N/A
0→34.00	433.60	5.34	199.34	2.99	115.27	2.15

Table 3. Response times for 3.1×10^{-5} M HPTS and 3.1×10^{-5} M NR in phosphate buffer at pH 7.0.

dCO ₂ Change (mM)	HPTS Response Time (min)	NR Response Time (min)
0.00→0.68	4.0	1.0
0.68→2.04	3.0	2.0
2.04→3.40	3.0	0.5
3.40→34.0	2.0	0.5
34.0→0.00	30.0	20.0

Changes in signal drift with respect to different concentrations of dCO₂ of the NR solution compared to the HPTS solution as well as the percent (%) emission signal change data for both NR and HPTS and at any given dCO₂ concentration there was less percent signal change for NR than HPTS (Table 4). For example, between the first and fourth N₂ cycle NR drifted down 24.2% percent while in contrast, HPTS drifted up by 13.5% and between the first and third 100% CO₂ cycle NR drifted up only 2.35% whereas HPTS drifted up to a much greater extent (43.7%). Further, it was clear that the NR exhibited enhancement in emission with increased carbon dioxide concentration while HPTS emission was

quenching with respect to increased dCO₂ concentration at 455 nm excitation. In short, an increase in CO₂ concentration resulted in emission enhancement and thereby minimized noise-related issues in the NR system compared to HPTS. Several previous studies have shown that modifications or different formulations of HPTS can exhibit significant variations in sensitivity, response time, and stability [1,7,12]. Yet, even without optimization, and under similar experimental conditions, HPTS exhibited higher sensitivity compared to the NR solution, however, the NR solution showed several other advantages over HPTS with respect to response time and signal drift. Therefore, from these results, we suggest that chemical modification of the NR molecule or variation of the formulation of the NR solution will result in a highly efficient dCO₂ sensor equal or better than that of HPTS [1,7]. Complete fluorescence data for these studies is given in Figure S5.

Table 4. Comparisons of drift between NR and HPTS showing the % signal change using the same dCO₂ concentration of two cycles, 0 mM (N₂*) and 34.0 mM (CO₂*). Comparisons were also made between the first cycle and the last cycle to show overall drift. Figure S4 contains complete fluorescence data.

Fluorescent Molecule	% Signal Change (%Δ)			
	1-N ₂ →2-N ₂	2-N ₂ →3-N ₂	3-N ₂ →4-N ₂	1-N ₂ →4-N ₂
NR	−11.8	−4.3	−6.6	−24.2
HPTS	4.2	7.2	1.6	13.5
	1-CO ₂ →2-CO ₂	2-CO ₂ →3-CO ₂	1-CO ₂ →3-CO ₂	
NR	−3.05	0.68	−2.35	
HPTS	31.0	9.7	43.7	

Calibration curves were derived for emission changes (%Δ) for data from the fluorometer and microscope, I/I_0 values were plotted vs. dCO₂ concentrations (Figure 9A). The best fit for the relationship between emission signal changes and dissolved CO₂, was found to be an exponential growth equation as determined by R² values (Table 5).

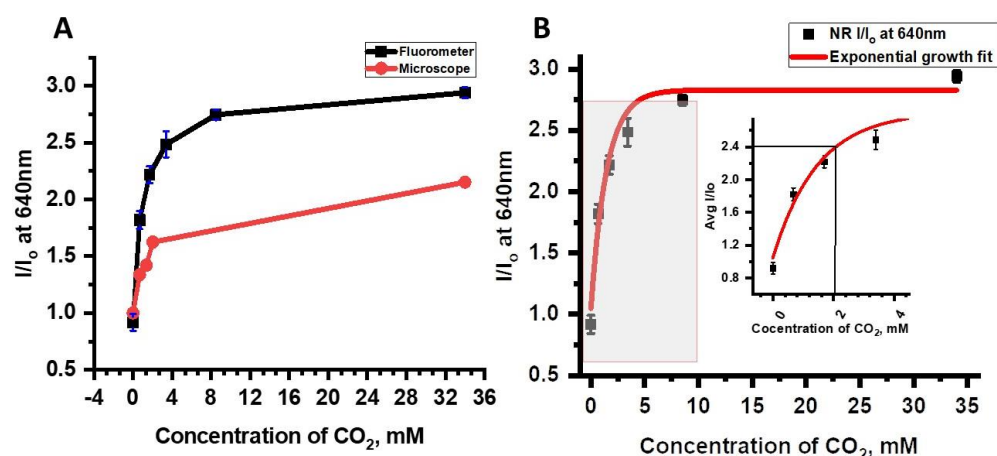


Figure 9. (A) Comparison of emission intensity changes for data acquired using a fluorometer and the microscope. The fluorometer data represents CO₂ gases at 0 mM, 0.68 mM, 2.04 mM, 3.4 mM and 34.0 mM concentrations, the microscope data represents CO₂ gases at 0 mM, 0.68 mM, 1.36 mM, 2.04 mM and 34.0 mM concentrations. (B) Calibration curve depicting the Limit of Detection (LoD) for the NR buffer solution purged with different concentrations of CO₂ and N₂ gases at pH 7.3 buffer solution. The data points are extracted from the absorption data which can be found in Figure S6. The arrow in the inset points is at the LoD value for the NR system.

Table 5. Exponential equations for luminescence intensity changes in dCO₂ concentration for microscope and fluorometer studies.

	Equation	R ²
dCO ₂ concentration (Microscope)	$y = -1.12e^{(x/-2.55)} + 2.15$	0.98
dCO ₂ concentration (Fluorometer)	$y = -1.79e^{(x/-1.35)} + 2.84$	0.97

Figure 9B provides the measurements for the calculation of the limit of detection for the NR solution when it was purged with different CO₂ and N₂ gases using Equation (1),

$$\text{LoD} = 3 \times S_{y/x} / m \quad (1)$$

where, ' $S_{y/x}$ ' is the Residual Standard Deviation and ' m ' is the slope of the calibration curve [26]. The LoD was calculated using the fluorescence vs. CO₂ concentration plot followed by linear regression analysis. The resulting slope and residual standard deviation were then substituted in the above equation to get the LoD that was determined to be 2.11 mM dCO₂ concentration for which the signal-to-noise ratio (I/I_0) was found to be 2.398. The regression analysis is provided in Table S2.

In summary, results from this comprehensive study provide evidence that NR may be used as a sensor to detect changes in CO₂ levels in the environment and may have the potential for measuring intracellular CO₂ levels within for biological analysis. The equilibrium concentration of bicarbonate (HCO₃[−]), carbonates (CO₃^{2−}) and dCO₂ in human blood is determined to be ~1.2 mM from the Henderson-Hasselback equation [7]. At this CO₂ concentration and using data from Figure 9, NR emission intensity would increase by 29.8% when using an epifluorescent microscope and by 126.07% using the fluorometer, therefore, it is probable that the percent signal change values can be easily differentiated from any background noise and even from high CO₂ concentrations in the medium, such as found in human blood. One of the largest disadvantages in Severinghaus electrodes for human blood analysis of dissolved carbon dioxide is the inability for continuous monitoring. Neutral Red has already shown the ability to stain lymphocytes of human blood [27]. Optical sensors respond to pH changes due to changes in CO₂ concentrations in the medium, allows for continuous signal monitoring. Response times, and ionic buffer strength dependence would be important to consider for human blood analysis [28]. In addition, the strong red emission and visible excitation offer numerous opportunities in the future for investigating the potential use of the NR to determine CO₂ concentrations in vitro or in vivo. When considering in vitro studies, it is important to note that neutral red has shown, when in concentrations smaller than 10^{−4} M, it can intercalate with DNA and result in chromatin fluorescence [15,29]. Although, in vivo sensing studies must consider neutral red's ability to absorb into acidic organelles, such as lysosomes [14,18]. Neutral Red also acts as a ligand upon complexation to riboflavin-binding protein [30]. Based on this information from literature, optimization of NR formulation is required for overcoming interactions and interference while working with biological components, as expected. However, the strong red emission and visible excitation of the NR system should overcome any background autofluorescence from different biological components that are generally expected to emit in the UV, near-UV, blue and green regions.

4. Conclusions

While NR has been known in the past primarily as a biological cellular staining agent, results from the present study were the first to demonstrate NR's ability to exhibit pH-induced emission and absorbance changes when exposed to different concentrations of dissolved CO₂. While NR has dual excitations at 455 nm and 540 nm with a single emission peak centering around 640 nm, in contrast to many popular CO₂ sensitive optical sensors, NR exhibited increased emission intensity with increases in dCO₂ concentrations. An added advantage of the NR system is that it has an emission wavelength that is

significantly red-shifted compared to the most established pH-induced, fluorescent CO₂ sensors in use (e.g., HPTS). This singular property of NR along with several others such as, a neutral detection range, miscibility in a phosphate buffer, low toxicity and significant emission intensity increases at concentrations of dCO₂ representative of human blood, shows that NR exhibits promising potential for sensing and detecting dCO₂ changes within a biological system for biomedical applications. In addition, from the results of this study, it was clear that NR had response times between 30 s and 1 min with maximum reversibility times of 20 min and NR also exhibited a 199.34% signal change in emission intensity and a 433.60% signal change in absorbance between pure N₂ and 100% CO₂ with full reversibility as well as exhibiting zero sensitivity to dissolved O₂. When these characteristics were benchmarked against HPTS, NR had better response and reversibility times with higher consistency in signal intensity over three cycles of response to different CO₂ concentrations. In the future, optimization of NR for enhancing the stability through polymerization or embedding within a matrix medium will be necessary. Based on results from the present study the potential for the future development of a fiber-optic sensor using NR is, therefore, possible, and even encouraged because the optical setup would be cheaper if visible light could be used instead of ultraviolet light for excitation wavelengths [1]. Further studies to determine the use and efficiency of NR as a CO₂ sensor in biological systems (e.g., in human blood) will be invaluable because of NR's low toxicity and lack of interference with the blue emission of cellular organelles [16–18]. The work herein suggests that NR can be applied for sensing in any biological system or biological process that exhibits CO₂ concentration range greater than 2.11 mM.

Supplementary Materials: The following are available online at <https://www.mdpi.com/article/10.3390/chemosensors9080210/s1>, Figure S1. Chemical structure of HPTS molecule showing pKa structural variations at equilibrium. Figure S2. (A) Excitation and emission studies of HPTS in different pH phosphate buffer media ranging from 5.9 to 8.2. (B) The color of the solutions depicted in the picture, TOP: Under ambient light and BOTTOM: Under UV irradiation Figure S3. Setup for the epifluorescence microscope. The components are labeled as 1. Zeiss Axio Observer (CAN-BUS) inverted microscope, 2. Power Supply, 3. Definite Focus module, 4. Temperature module, 5. CO₂ module, 6. O₂ module, 7. Heating device/humidity, 8. 100% CO₂ cylinder, 9. 100% N₂ cylinder, 10. Incubator chamber Table S1. Carbon dioxide sensitivity numbers obtained from absorption and fluorescence measurements are compared. Fluorescence measurements are collected using spectrophotometer (fluorescence), and epifluorescent microscope (fluorescence*) Figure S4. The results showing no sensitivity when NR in phosphate buffer media is purged with O₂ Figure S5. Carbon dioxide sensitivity purging cycles of HPTS and NR in phosphate buffer media Figure S6. Linear fit analysis for the calculation of residual standard deviation and slope Table S2. Linear fit analysis for the calculation of residual standard deviation and slope.

Author Contributions: Conceptualization, S.B.M. and I.H.v.H.; project administration, S.B.M., I.H.v.H. and M.A.O.; supervision, S.B.M., I.H.v.H. and M.A.O.; investigation, S.B.M., I.H.v.H., M.N.E., S.K.S. and L.M.C.; methodology, S.B.M. and I.H.v.H.; experiments, data generation, and analysis, M.N.E., S.K.S., L.M.C., I.H.v.H. and S.B.M.; resources, S.B.M., I.H.v.H. and M.A.O.; Writing—Original draft preparation, M.N.E., S.B.M. and I.H.v.H.; Writing—Review and editing, M.N.E., S.B.M., I.H.v.H., S.K.S. and M.A.O.; funding and acquisition, S.B.M., I.H.v.H. and M.A.O. S.K.S. and M.N.E. are equal contributing first authors. All authors have read and agreed to the published version of the manuscript.

Funding: This work was primarily funded by a 2018 UNT-COS Seed Grant (822402) to Ione Hunt von Herbing and Sreekar B. Marpu, whereas peripheral support by the Welch Foundation (B-1542) and the National Science Foundation (CHE-1413641) to Mohammad A. Omary on luminescent materials development and/or applications is also acknowledged.

Data Availability Statement: Data is contained within the article or supplementary materials. The link to supplementary materials can be found here.

Acknowledgments: We are grateful for help with some measurements from Naman Bhasin and Tejas Alankar, TAMS research students at UNT. Data collected for this paper form part of an MS thesis for Megan N. Ericson and PhD thesis for Sindhu K. Shankar.

Conflicts of Interest: The authors declare no conflict of interest.

References

1. Lakowicz, J.R.; Geddes, C.D. *Topics in Fluorescence Spectroscopy, Advanced Concepts in Fluorescence Sensing Part A: Small Molecule Sensing*; Springer: New York, NY, USA, 2005; Volume 9.
2. Mou, D.G. Process Dynamics, Instrumentation and Control. *Biotech. Adv.* **1983**, *1*, 229–245. [CrossRef]
3. Rooney, M.L. *Active Food Packaging*; Blackie Academic & Professional: London, UK, 1995.
4. United States Geological Survey. Science for a Changing World: Dissolved Oxygen and Water. Available online: https://www.usgs.gov/special-topic/water-science-school/science/dissolvedoxygen-and-water?qt-science_center_objects=0#qt-science_center_objects (accessed on 1 August 2019).
5. Lake, C.L. *Clinical Monitoring*; W.B. Saunders Co.: Philadelphia, PA, USA, 1990.
6. Helenius, I.T.; Krupinski, T.; Turnbull, D.W.; Gruenbaum, Y.; Silverman, N.; Johnson, E.A.; Sporn, P.H.S.; Sznajder, J.I.; Beitel, G.J. Elevated CO₂ suppresses specific *Drosophila* innate immune response and resistance to bacterial infection. *Proc. Natl. Acad. Sci. USA* **2009**, *106*, 18710–18715. [CrossRef] [PubMed]
7. Dakin, J.; Culshaw, B. *Optical Fiber Sensors*; Artech House: Boston, MA, USA; London, UK; Norwood, MA, USA, 1997; Volume IV, Chapter 8; pp. 53–107.
8. Lide, D.R. *CRC Handbook of Chemistry and Physics*, 84th ed.; CRC Press: Boca Raton, FL, USA, 2004.
9. Severinghaus, W.; Bradley, A.F. Electrodes for blood pO₂ and pCO₂ determination. *Appl. Physiol.* **1958**, *13*, 515–520. [CrossRef] [PubMed]
10. Jensen, M.A.; Rechnitz, G.A. Response time characteristics of the pCO₂ electrode. *Anal. Chem.* **1979**, *51*, 1972–1977. [CrossRef]
11. Rhys, A.T. *An Introduction to Fluorescence Spectroscopy*; PerkinElmer: Beaconsfield, UK, 2000.
12. Han, J.; Burgess, K. Fluorescent Indicators for Intracellular pH. *Chem. Rev.* **2009**, *110*, 2709–2728. [CrossRef] [PubMed]
13. Sousa, C.; Sa e Melo, T.; Geze, M.; Gaullier, J.M.; Maziere, J.C.; Santus, R. Photochem. *Photobiol.* **1996**, *63*, 601–607. [CrossRef] [PubMed]
14. Kirk, P.W. Neutral Red as a Lipid Fluorochrome. *Stain. Technol.* **1970**, *5*, 1–4. [CrossRef] [PubMed]
15. Espelösin, R.H.; Stockert, J.C. Neutral Red Fluorescence of Chromatin: Specificity and Binding Mechanism. *Z. Nat. C* **1982**, *37*, 139–141. [CrossRef] [PubMed]
16. Roshchina, V.V. Vital Autofluorescence: Application to the Study of Plant Living Cells. *Int. J. Spectrosc.* **2012**, *2012*, 124672. [CrossRef]
17. Croce, A.C.; Bottioli, G. Autofluorescence spectroscopy and imaging: A tool for biomedical research and diagnosis. *Eur. J. Histochem.* **2014**, *58*, 2461. [CrossRef] [PubMed]
18. Repetto, G.; del Peso, A.; Jorge, L. Neutral red uptake assay for the estimation of cell viability/cytotoxicity. *Zurita. Nat. Protoc.* **2008**, *3*, 1125–1131. [CrossRef]
19. Kastury, F.; Juhasz, A.; Beckmann, S.; Manefield, M. Ecotoxicity of neutral red (dye) and its environmental applications. *Ecotoxicol. Environ. Saf.* **2015**, *122*, 186–192. [CrossRef]
20. The University of Tennessee, Knoxville; The Institute of Environmental Modeling. Alternative Routes to Quantitative Literacy for the Life Sciences. Maintaining Cellular Conditions: pH and Buffers. Available online: <http://www.tiem.utk.edu/~jgross/bioed/webmodules/phbuffers.html> (accessed on 17 July 2019).
21. *Axio Observer Operating Manual*; Version 5; Carl Zeiss MicroImaging GmbH: Oberkochen, Germany, 2006.
22. Levine, I.N. *Physical Chemistry*, 4th ed.; Phase Rule, Phase Diagrams; McGraw-Hill: New York, NY, USA, 1995.
23. Carl Zeiss Microscopy. Overview of Filter Sets. Available online: <https://www.micro-shop.zeiss.com/en/us/shop/filter/Assistant/filtersets/> (accessed on 1 October 2019).
24. Schneider, C.A.; Rasband, W.S.; Eliceiri, K.W. NIH Image to ImageJ: 25 years of image analysis. *Nat. Methods* **2012**, *9*, 671–675. [CrossRef]
25. Bartels, H. Blood oxygen dissociation curves: Mammals. In *Respiration and Circulation*; Altman, P.L., Ditter, S.W., Eds.; Bethesda, Md., Federation of American Societies for Experimental Biology: Rockville, MD, USA, 1971.
26. Elmorsi, T.M.; Aysha, T.S.; Machalický, O.; Mohamed, M.B.; Bedair, A.H. A dual functional colorimetric and fluorescence chemosensor based on benzo[f]fluorescein dye derivatives for copper ions and pH; kinetics and thermodynamic study. *Sens. Actuators B Chem.* **2017**, *253*, 437–450. [CrossRef]
27. Hempelmann, L.H.; Knowlton, N.P. The Nature of Neutral Red Staining Refractive Particles in the Lymphocytes of the Blood of Normal Humans. *Blood* **1953**, *8*, 524–535. [CrossRef] [PubMed]
28. Jin, W.; Jiang, J.; Song, Y.; Bai, C. Real-time monitoring of blood carbon dioxide tension by fluorosensor. *Respir. Physiol. Neurobiol.* **2012**, *180*, 141–146. [CrossRef] [PubMed]
29. Moghaddam, F.G.; Kompany-Zareh, M.; Gholami, S. Study of neutral red interaction with DNA by resolution of rank deficient multi-way fluorescence data. *J. Pharm. Biomed. Anal.* **2012**, *70*, 388–395. [CrossRef]
30. Chenprakhon, P.; Sucharitakul, J.; Panijpan, B.; Chaiyen, P. Measuring Binding Affinity of Protein–Ligand Interaction Using Spectrophotometry: Binding of Neutral Red to Riboflavin-Binding Protein. *J. Chem. Educ.* **2010**, *87*, 829–831. [CrossRef]